Entanglement between particle partitions in itinerant many-particle states

Masudul Haque[1]**, O S Zozulya**[2] **and K Schoutens**[2]

[1] Max-Planck Institute for the Physics of Complex Systems, Nöthnitzer Str. 38, 01187 Dresden, Germany
[2] Institute for Theoretical Physics, University of Amsterdam, Valckenierstraat 65, 1018 XE Amsterdam, The Netherlands

Abstract
We review 'particle-partitioning entanglement' for itinerant many-particle systems. This is defined as the entanglement between two subsets of particles making up the system. We identify generic features and mechanisms of particle entanglement that are valid over whole classes of itinerant quantum systems. We formulate the general structure of particle entanglement in many-fermion ground states, analogous to the 'area law' for the more usually studied entanglement between spatial regions. The basic properties of particle entanglement are first elucidated by considering relatively simple itinerant models. We then review particle-partitioning entanglement in quantum states with more intricate physics, such as anyonic models and quantum Hall states.

PACS numbers: 03.67.Mn, 03.75.Gg, 64.70.Tg, 71.10.−w

(Some figures in this article are in colour only in the electronic version)

1. Introduction

Bipartite entanglement in many-particle systems, i.e. the entanglement between one part (A) of a system and the rest (B), has grown into a widely studied topic in the last few years. Usually, the partitioning is spatial, so that A is a collection of lattice sites or is a connected region of space. In this article, we will consider an alternate form of partitioning, namely *particle partitioning*. With the wavefunction expressed in first-quantized form, one can meaningfully partition particles rather than space, and calculate entanglements between subsets of particles. Since each particle has a label in first-quantized wavefunctions, indistinguishability does not preclude well-defined subsets of particles. Note that, with such partitioning, A or B does not correspond to connected regions of space. Also note that particle partitioning is only defined in itinerant systems where the particles hop, and thus has no meaning for pure spin models.

Particle-partitioning entanglement is generally quite different from the entanglement between spatial partitions of the same system, and also provides a distinct set of physical insights compared to the more standard spatial partitioning entanglement calculations. Particle entanglement provides a novel and unique perspective on the structure of itinerant many-particle wavefunctions.

Given a partitioning, the entanglement can be quantified using various measures. The basic quantity is the *reduced density matrix* of the A partition, $\rho_A = \text{tr}_B \, \rho$, obtained by tracing out B degrees of freedom. We assume the system to be in a pure state, described by density matrix $\rho = |\psi\rangle\langle\psi|$. Various entanglement quantifiers can then be extracted from ρ_A. We will mostly confine ourselves to the entanglement entropy S_A, defined as $S_A = -\text{tr}[\rho_A \ln \rho_A]$. We will also restrict ourselves to zero temperatures, i.e. to entanglement in the ground state of itinerant systems.

Brief history. Several pieces of work explored simple versions of particle-partitioning entanglement between identical quantum particles, even before the concept was carefully distinguished from spatial entanglement [1–7]. The relationship between quantum indistinguishability and entanglement was studied for two fermions in [1] and for two bosons in [2]. Particle entanglement was studied in [4, 6] in somewhat more complicated systems.

A careful distinction with spatial entanglement, and a comparison between the two types of partitioning, appears in [8, 9], in the context of fractional quantum Hall (FQH) states. Particle partitioning is tempting in entanglement considerations for FQH states because FQH model wavefunctions (e.g. Laughlin states) are often written in first-quantized form where the particles have explicit labels. Thus, particle-partitioning entanglement in FQH states has also been computed in [4, 7].

In [8, 9] and in work reported since then [10–12], particle entanglement has been shown to be a promising novel measure of correlations. In fractional quantum Hall states this type of entanglement reveals the *exclusion statistics* inherent in excitations of such states [8, 9]. Similar insight arises from particle entanglement calculations in the Calogero–Sutherland model [11]. For one-dimensional anyon states, particle-partitioning entanglement is found to be sensitive to the anyon statistics parameter [12, 13].

This review. Clearly, entanglement between particles in itinerant systems is a promising new concept, potentially useful for describing subtle correlations and the interplay between statistics and interaction effects. A broad study of the concept and its utility is obviously necessary. In this review, we will survey the results that are available until now. We will focus in particular on common features and on results of wide generality, that provide insights into classes of quantum itinerant systems.

The present review is solely concerned with particle-partitioning entanglement in itinerant many-particle systems. We will therefore not discuss entanglement between spatial partitions, or any other kind of entanglement. Reviews of other types of entanglement can be found, e.g. in [14, 15]. The other reviews of this special issue provide more recent and more condensed-matter-oriented perspectives on entanglement in many-particle states.

The target audience for this review is condensed matter physicists interested in various possible kinds of entanglement in many-particle wavefunctions. As such, other than using the definition of the entanglement entropy S_A, we do not treat or use any quantum information theory topics. A recent review of quantum entanglement was provided in [16] from that perspective. It is of course not possible to make a review of the present type completely self-contained since we cannot introduce in detail each of the several models and states considered here. We therefore assume familiarity with several classes of many-particle states or models. Only minimal motivational background is provided for each model. The topic here is particle-

partitioning entanglement and not the individual models. We expect that the typical theorist practicing condensed matter will indeed be familiar with most of the many-particle models and states employed.

We start in section 2 by working out in detail an elementary example of particle partitioning, contrasted to spatial partitioning of the same quantum state. The fact that entanglement depends crucially on the type of partitioning is perhaps not as widely appreciated as it should be; we hope that a detailed example helps clarify the concept of particle partitioning. In section 3 we present some generic results and intuitions, before moving on to specific systems in the following sections.

Sections 4–6 consider respectively bosons, fermions and anyons, and review numerical and analytical results in order to provide an overview of various mechanisms for particle-partitioning entanglement. We then turn to more unusual many-particle states: section 7 reviews results for fractional quantum Hall states and section 8 for the Calogero–Sutherland models.

2. An elementary example

The concept of particle partitioning causes enough confusion to justify using a very simple example to illustrate in detail the definition and its difference from spatial partitioning. Readers comfortable with the concept may safely skip this section.

We imagine two (spinless) fermions in three sites (or orbitals), which we label α, β, γ. We will use the wavefunction

$$|\psi\rangle = \left(a_1 c_\alpha^\dagger c_\beta^\dagger + a_2 c_\beta^\dagger c_\gamma^\dagger\right)|\text{vacuum}\rangle = a_1|110\rangle + a_2|011\rangle.$$

For usual spatial partitioning, we can consider for example partition A to consist of site α only. Then the reduced basis for A consists of the α microstates $|0\rangle$ and $|1\rangle = c_\alpha^\dagger|0\rangle$, and the reduced density matrix in this basis is $\rho_A = \begin{pmatrix} |a_2|^2 & 0 \\ 0 & |a_1|^2 \end{pmatrix}$.

One could also take A to contain sites α and β. Then the reduced basis for A contains four states, $|00\rangle$, $|01\rangle = c_\beta^\dagger|0\rangle$, $|10\rangle = c_\alpha^\dagger|0\rangle$ and $|11\rangle = c_\alpha^\dagger c_\beta^\dagger|0\rangle$, and in this basis

$$\rho_A = \begin{pmatrix} 0 & 0 & 0 & 0 \\ 0 & |a_2|^2 & 0 & 0 \\ 0 & 0 & 0 & 0 \\ 0 & 0 & 0 & |a_1|^2 \end{pmatrix}.$$

We next turn to particle partitioning, for which the wavefunction must be expressed in first-quantized form with explicit anti-symmetrization:

$$|\psi\rangle = a_1[\phi_\alpha(1)\phi_\beta(2) - \phi_\alpha(2)\phi_\beta(1)]/\sqrt{2} + a_2[\phi_\beta(1)\phi_\gamma(2) - \phi_\beta(2)\phi_\gamma(1)]/\sqrt{2}.$$

The particles (fermions) now have labels, so that we can consider the entanglement between particle 1 and particle 2. (Partition A contains particle 1.) Since particle 1 can be in any one of the three sites, the reduced basis for A can be labeled by the site labels, $|\alpha\rangle$, $|\beta\rangle$, $|\gamma\rangle$. The reduced density matrix is

$$\rho_A = \begin{pmatrix} |a_1|^2/2 & 0 & -a_1 a_2^* \\ 0 & 1/2 & 0 \\ -a_1^* a_2 & 0 & |a_2|^2/2 \end{pmatrix}.$$

From this simple example we already see that particle-partitioning entanglement is utterly different from spatial or site partitioning entanglement. A second lesson that emerges from

this example is that particle-partitioning entanglement is affected substantially by the (anti-) symmetrization which is explicit in first quantization. It is therefore no surprise that this type of entanglement is especially sensitive to quantum statistics.

3. General considerations

Before analyzing specific systems, we present some facts and conjectures broadly applicable to a variety of itinerant quantum many-particle states.

3.1. Bounds

A generic itinerant lattice system has N particles in L sites; we consider bosons or spinless fermions with $N \leqslant L$. In every case, a natural upper bound for S_n is provided by the (logarithm of the) size of the reduced density matrix $\rho_A = \rho_n$, i.e. the dimensions of the reduced Hilbert space of the A partition. This size is $\binom{L}{n} = C(L, n)$ for fermions and $C(L - 1 + n, n)$ for bosons. The actual rank of ρ_n can be much smaller due to physical reasons, so that the entanglement entropies are usually significantly smaller than the upper bounds, as we shall see in the examples we treat.

In a bosonic system, S_n can vanish since a Bose condensate wavefunction is simply a product state of individual boson wavefunctions, each identical. For fermions, however, anti-symmetrization requires the superposition of product states; for free fermions described by a Slater determinant wavefunction, this causes ρ_n to have $C(N, n)$ equal eigenvalues. This provides a nonzero lower bound for S_n in a fermionic system. To summarize,

$$\text{Bosons}: \quad 0 \leqslant S_n \leqslant \ln \binom{L - 1 + n}{n}, \tag{1}$$

$$\text{Fermions}: \quad \ln \binom{N}{n} \leqslant S_n \leqslant \ln \binom{L}{n}. \tag{2}$$

3.2. Standard form for fermions

For large fermion number, $N \gg 1$, we propose the following widely applicable form for the entanglement of $n \ll N$ fermions with the rest:

$$S_n(N) = \ln C(N, n) + \alpha_n + \mathcal{O}(1/N^\gamma) \tag{3}$$

$$= n \ln N + \alpha_n' + \mathcal{O}(1/N^\gamma), \tag{4}$$

with $\gamma > 0$. This form is suggested by results reported in [8–12]. For example, $\alpha_n = n \ln m$ for the Laughlin state at filling $\nu = 1/m$ [8]. The same standard behavior seems to hold for bosonic systems which lack macroscopic condensation into a single mode, e.g. bosonic Laughlin states [9], or hard-core repulsive bosons in one dimension [21]. Note that, for lattice sizes larger than N, the generic behavior (3) indicates that the entanglement entropy does not saturate the upper bound (1) or (2) obtained from the size of the reduced Hilbert space.

Subtle correlation and statistics effects can be contained in the behavior of the $\mathcal{O}(1)$ term α_n, and sometimes also the $\mathcal{O}(1/N^\gamma)$ term. To get some intuition about how such effects show up in α_n, we summarize the behavior of α_n for several kinds of states. For free fermions,
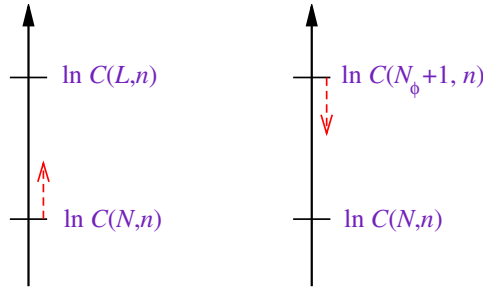
4

Figure 1. Lower and upper bounds for particle-partitioning entanglement in fermionic systems. Left: usual situation such as mobile fermions in a non-frustrated lattice. Right: fermions in a flat band or within a Landau level, with macroscopic degeneracy. Dashed arrows show the effect of turning on interactions.

for charge-ordered states of the spinless-fermion model (subsection 5.1, also [10]) and for Laughlin states (section 7 and [8, 9]), we have

$$\alpha_n(\text{FF}) = 0, \qquad \alpha_n(\text{CDW}) = \ln 2, \qquad \alpha_n(\text{Laughlin}) = n \ln m.$$

We note that states which are intuitively 'more nontrivially correlated' have stronger n-dependence in α_n. This strongly suggests that the α_n function is a measure of correlations in itinerant fermionic states. It is natural to conjecture that the linear-in-n behavior of α_n is symptomatic of intricately correlated states like quantum Hall states, and that in generic itinerant states α_n will have sub-linear dependences on n.

3.3. Exceptional case of macroscopic degeneracy

One has to treat with care the cases where the single-particle spectrum has a highly degenerate ground state with degeneracy larger than N. The case of fractional quantum Hall (FQH) states is one example that we will treat in detail in section 7. For FQH states, the appropriate Landau level is immensely degenerate and only partially filled. Another example is a macroscopically degenerate 'flat band' that is partially filled. Flat bands appear in the band structure of frustrated lattices (kagome, checkerboard, pyrochlore, etc), where one of the energy bands can be dispersion-free and have the same energy for all momentum; hence the name 'flat'. (See, e.g. [17] for a discussion of itinerant systems in flat-band situations due to lattice frustration.)

Denoting the degeneracy by $N_\phi + 1$ (FQH notation), we have the upper bounds

$$S_n \leqslant \ln \binom{N_\phi + 1}{n}, \qquad S_n \leqslant \ln \binom{(N_\phi + 1) + n - 1}{n},$$

respectively, for fermions and bosons, from Hilbert-space counting alone. This is very similar to the case of N particles in L sites, above. (The lower bounds are the same as before.) The difference is that for non-interacting particles in a flat band, S_n can be equal to the upper bound, whereas in the usual case it is equal to the lower bound. In this case of macroscopic degeneracy, interactions *reduce* the particle entanglement from the upper bound, as opposed to the conventional situation where interactions *raise* the particle entanglement from the lower bound. This is illustrated schematically in figure 1.

5

3.4. Generic mechanisms: Slater terms, fragmentation or absence of condensation and massive degeneracies

We summarize here the mechanisms through which an itinerant many-particle system can possess particle-partitioning entanglement. This provides intuition concerning what physical information is contained in the entanglement between particle partitions.

An ideal bosonic system is fully condensed in a single mode, and therefore has $S_n = 0$. Thus, for bosonic systems, particle entanglement is a measure of the *deviation* from Bose condensation. Interactions provide a simple mechanism for this—since an interacting Bose system is only partially condensed, it possesses nonzero particle entanglement. Another mechanism is low dimensionality; hard-core repulsive bosons living on a line (1D continuum; Lieb–Liniger model) do not condense. In addition, condensate fragmentation provides a second mechanism for nonzero S_n. Fragmentation is not as exotic a phenomenon as commonly perceived; in fact it provides a unifying perspective to describe Mott phases of bosons in lattice geometries [18]. Finally, one can also have $S_n \neq 0$ through quantum-mechanical superposition of condensates in different modes, i.e. Schrödinger cat states. In section 4, we will illustrate these situations through several examples.

For fermionic systems, fermionic statistics already provides a contribution $\ln C(N, n)$ to the particle-entanglement entropy—this is the value of S_n when the system wavefunction is a single Slater determinant. The excess particle entanglement over this amount tells us how far one has to go beyond a single Slater determinant in order to describe the physics of the system. In other words, the excess particle entanglement reflects loosely the number of Slater determinant terms of similar amplitudes that need to be combined to produce the system wavefunction.

The cases of macroscopic degeneracies require additional considerations. Particle entanglement can be large here due to the much larger Hilbert space available without paying an energy cost, so that ground state wavefunctions can involve much more than a single Slater determinant (fermions) or a few condensate modes (bosons).

3.5. Relationship with correlation functions

The purpose of this subsection is to clarify the relationship between particle-partitioning entanglement and more traditional condensed-matter quantities, namely correlation functions.

In the easiest case, $n = 1$, the one-particle entanglement entropy S_1 can be obtained from the one-particle correlation functions or the single-particle state occupancies. For example, for one-dimensional translationally invariant systems, S_1 can be expressed through momentum occupation numbers. The momentum occupation numbers are Fourier transforms of the reduced density matrix: $c(k) = L^{-1} \int_0^L \mathrm{d}x\, \rho_1(x) \cos(2\pi k x / L)$, with L being the size of the system. Then

$$S_1 = -\sum_k c(k) \ln c(k).$$

More generally, for $n > 1$ it is intuitively clear that the elements of the reduced density matrices are proportional to correlation functions. We write down the precise relationship for a 1D continuum case:

$$\rho_n(\vec{x}_n, \vec{y}_n) = \frac{(N-n)!}{N!} \langle \Psi | \phi^\dagger(x_1) \cdots \phi^\dagger(x_n) \phi(y_n) \cdots \phi(y_1) | \Psi \rangle.$$

where the 'vectors' $\vec{x}_n$, $\vec{y}_n$ encode coordinates of n particles, and

$$\rho_n(\vec{x}_n, \vec{y}_n) = \int dz_{n+1} \cdots dz_N \Psi^*(x_1, \ldots, x_n, z_{n+1}, \ldots, z_N) \Psi(y_1, \ldots, y_n, z_{n+1}, \ldots, z_N).$$

The modification to lattice cases or higher dimensions is obvious.

4. Bosonic systems: role of condensation

In this section we illustrate the interplay between particle-partitioning entanglement and Bose condensation, through several example models. First, considering a two-site Bose–Hubbard model, we demonstrate nonzero particle-partitioning entanglement through *condensate fragmentation* and the formation of *Schrödinger cat states*. Next, consideration of a lattice boson model and the continuum Lieb–Liniger model reveals bosonic particle entanglement due to partial condensation and absence of condensation, respectively.

4.1. Toy model: two-site Bose–Hubbard

Following [10], we consider N bosons on a two-site 'lattice', subject to a Bose–Hubbard model Hamiltonian. The Hamiltonian is

$$\hat{H} = -\left(\hat{b}_1^\dagger \hat{b}_2 + \hat{b}_2^\dagger \hat{b}_1\right) + \tfrac{1}{2}U\left(\hat{b}_1^\dagger \hat{b}_1^\dagger \hat{b}_1 \hat{b}_1 + \hat{b}_2^\dagger \hat{b}_2^\dagger \hat{b}_2 \hat{b}_2\right). \tag{5}$$

We label the N-boson basis states by site occupancies, i.e. as $|N_1, N_2\rangle = |N_1, N - N_1\rangle$.

For $U = 0$, the system is a non-interacting Bose condensate, with each boson packed into the single-particle state $\frac{1}{\sqrt{2}}(|1\rangle + |2\rangle)$. In the $U \to +\infty$ case, the system is a Mott insulator, with half the particles in site 1 and the other half in site 2, $|N/2, N/2\rangle$. Such a state is simple in the 'site' basis (second-quantized wavefunction), but involves symmetrization in the 'particle' basis (first-quantized wavefunction), leading to nonzero particle-entanglement entropy.

Finally, the $U \to -\infty$ limit involves all particles in either site 1 or site 2. The ground state is a linear combination of these two possibilities, $\frac{1}{\sqrt{2}}(|0, N\rangle + |N, 0\rangle)$, which for large N is a macroscopic 'Schrödinger cat' state. Such a state is somewhat artificial because an infinitesimal energy imbalance between the two states will 'collapse' this state. For example, a 'symmetry-breaking' term of the form $\epsilon \hat{b}_1^\dagger \hat{b}_1$, added to the Hamiltonian (5), would favor site 2 and destroy the cat state. The resulting state is a product state with zero particle entanglement.

For the simplest case of two bosons, there is only one way of partitioning ($n = 1$), so the only S_n is S_1. We expect $S_1 = 0$ at $U = 0$, and maximal entanglement $S_1 = \ln 2$ for both 'Mott' state at $U = +\infty$ and the 'Schrödinger cat' state at $U = -\infty$. The Hilbert space is small; one can diagonalize the problem and calculate S_1 analytically as a function of U. One finds $S_1(U) = S_1(-U)$, interpolating smoothly between zero and $\ln 2 \simeq 0.6931$ in both positive and negative directions (figure 2(*a*)).

Figure 2(*a*) also demonstrates the fragility of the cat state by showing the effect of an $\epsilon \hat{b}_1^\dagger \hat{b}_1$ term (dashed curve). There is no appreciable effect for $U > 0$, but for $U < 0$ the cat state is destroyed and we get $S_1 \to 0$ for $U \to -\infty$.

For $N > 2$ bosons, it is meaningful to study S_n with $n > 1$. The n-particle reduced Hilbert space has dimension $n + 1$; the reduced-space basis states can be labeled by the number of A bosons in site 1. In the Mott state $|N/2, N/2\rangle$, only the diagonal elements of ρ_n are nonzero and they are all equal; hence $S_n(U \to \infty) = \ln(n + 1)$. In the cat state, only two elements are nonzero, both on the diagonal; hence, $S_n(U \to -\infty) = \ln 2$, independent of n. Figure 2(*b*) demonstrates, via calculation from wavefunctions obtained by numerical diagonalization, that S_n increases to $\ln(n + 1)$ and $\ln 2$ in the $U \to \pm\infty$ limits. On the negative side, the change
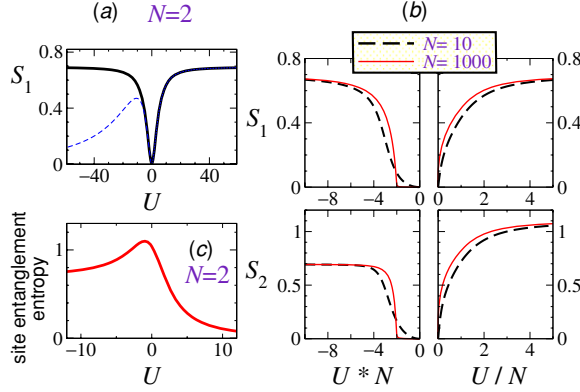
Figure 2. (*a, b*) Particle-partitioning entanglement for bosons in the ground state of a two-site lattice model with on-site repulsion. (*a*) Two bosons. Solid curve is for the basic Bose–Hubbard model. Dashed curve illustrates fragility of 'cat' state via a $\epsilon \hat{b}_1^\dagger \hat{b}_1$ term ($\epsilon = 0.1$). (*b*) 1-particle and 2-particle entanglement entropies for $N = 10$ (1000) bosons in two sites. Note different units for positive and negative U. (*c*) Entropy of spatial entanglement between the two sites ($N = 2$).

occurs sharply (around $U = -2/N$); the ground state remains nearly unentangled between $U = 0$ and $U = -2/N$.

Both $\rho_n(U)$ and $S_n(U)$ can be understood in greater detail using available approximations for the two-site model [18]; a description is given in [10].

To summarize, in the two-site Bose–Hubbard model the Mott state for $U > 0$ and Schrödinger cat state for $U < 0$ both possess the particle entanglement. This particle entanglement in the two regimes has different physical origins: the physics of fragmented condensation for $U > 0$ and that of Schrödinger cat states for $U < 0$.

Comparison with spatial entanglement.   In figure 2(*c*) we plot the entropy of entanglement between the two sites, i.e. the 'spatial' entanglement. The spatial entanglement is zero in the Mott regime of $U \to +\infty$, where the wavefunction is a product state in the second-quantized wavefunction. (Symmetrization plays no role.) In the Schrödinger cat regime of $U \to -\infty$, the spatial entanglement is $\ln 2$ like the particle-partitioning entanglement. In the Bose condensate regime (small U), the spatial entanglement between sites is large, and for $N = 2$ peaks at $\ln 3$ at some small negative U. Thus, particle partitioning and spatial partitioning lead to very different entanglements, except for the $U \to -\infty$ limit.

4.2. Hard-core bosons on one-dimensional lattice

Having considered fragmentation and cat states through the two-site model, we now turn to imperfect or partial condensation. One way to access such a state is through the model of hard-core bosons on a 1D lattice (forbidden multiple occupancy, $U = \infty$) with attractive nearest-neighbor interaction V:

$$H = -\sum_i \left(c_i^\dagger c_{i+1} + c_{i+1}^\dagger c_i \right) + V \sum_i n_i n_{i+1} + U \sum_i n_i (n_i - 1),$$

with $U \to \infty$. We consider N bosons in L sites, subject to periodic boundary conditions. This is closely related to the spinless fermion model treated later in subsection 5.1.

The point $V = -2$ has a 'simple' ground state known exactly [26]. This wavefunction is a symmetric equal-amplitude combination of all possible $C(L, N)$ arrangements of bosons. The exact wavefunction can be exploited to yield [10]

$$S_n = \nu n \ln N + \mathcal{O}(N^0),$$

where $\nu = N/L$ is the filling fraction. A natural interpretation is that the pre-factor represents the un-condensed fraction. Whether this is generic for bosonic systems with partial condensation remains an open question.

Details for $n = 1$. The one-particle reduced density matrix is diagonal in the momentum representation, and has values

$$\langle k|\rho_1|k\rangle = (N-1)/[L(L-1)] \qquad \text{for} \quad k \neq 0$$
$$\langle k|\rho_1|k\rangle = (L-N+1)/L \qquad \text{for} \quad k = 0.$$

In the limit $L \to \infty$ (with fixed filling $\nu = N/L$), the $k = 0$ eigenvalue becomes macroscopic at the expense of the others, indicating off-diagonal long-range order [19] and partial condensation with condensate strength $1 - \nu$.

Other cases of imperfect condensation. Interacting bosons in three dimensions also have partial condensation; it would be interesting to calculate S_n for such a model.

4.3. Lieb–Liniger bosons

The generic 1D continuum boson model with repulsive contact interactions (Lieb–Liniger model [20]) does not possess Bose condensation, and instead the particles fill up individual-particle levels just as fermions do. (In the Bethe ansatz these levels are labeled by rapidities.) One can thus expect a leading $S_n \sim n \ln N$ behavior as for fermions. Currently available evidence strongly suggests this to be the case.

For $n = 1$, the results of [12] (reviewed in section 6) allow us to infer a leading $\ln N$ for the large-interaction limit, also known as the Tonks–Girardeau limit. In addition, unpublished numerical results indicate that the behavior $S_1 \sim \ln N$ holds for any nonzero interaction [21].

5. Fermionic systems: anti-symmetrization and correlations

Following [10], in 5.1 we use numerical calculations of the spinless fermion chain with nearest-neighbor interactions (*t–V* model), one of the basic models of correlated-electron physics, to illustrate particle entanglement in fermionic systems. Other systems are commented on in 5.2.

5.1. Spinless fermions in one dimension

We consider N spinless fermions on an L-site chain with periodic boundary conditions:

$$H = -\sum_i \left(c_i^\dagger c_{i+1} + c_{i+1}^\dagger c_i\right) + V \sum_i n_i n_{i+1}.$$

Through a Jordan–Wigner transformation, this model can be mapped to the anisotropic Heisenberg (*XXZ*) spin chain model with anisotropy parameter $\Delta = V/2$.

For $V = 0$ (free fermions), the ground state is simple in terms of momentum–space modes: a Slater determinant of the N fermions occupying the N lowest-energy modes. The n-particle reduced density matrix has $C(N, n)$ equal eigenvalues, so that $S_n = \ln[C(N, n)]$, independent of the lattice size L.
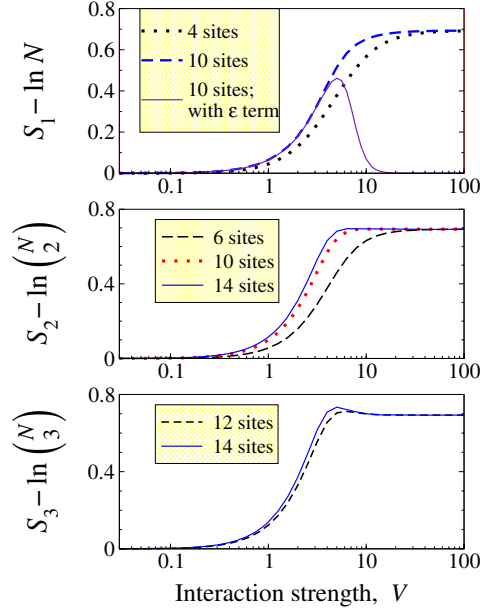
Figure 3. $n = 1$, $n = 2$ and $n = 3$ entanglement entropy in half-filled *t-V* model ($N = L/2$). The free-fermion contribution $\ln[C(N, n)]$ has been subtracted off. The $n = 1$ plot also displays the effect of a symmetry-breaking $\epsilon c_1^\dagger c_1$ term, with $\epsilon = 0.1$. Inset: position of the maximum as function of ϵ.

Half-filling. For repulsive interactions at half filling $\left(N = \frac{1}{2}L\right)$, this model has a quantum phase transition at $V = 2$, from a Luttinger-liquid phase at small V to a charge density wave (CDW) phase at large V. This mirrors the well-known transition between gapless XY and gapped Ising phases in the *XXZ* model at the Heisenberg point $\Delta = 1$ [22].

For $N = \frac{1}{2}L$, the ground state and hence particle entanglement can be simply understood in the infinite-V limit. The ground state is an equal superposition of two 'crystal' states, and each of them gives a separate contribution to the reduced density matrix. The reduced density matrix has rank $2C(N, n)$ and equal eigenvalues: $S_n = \ln[2C(N, n)]$. In the notation of equation (3), the sub-leading term α_n interpolates between $\alpha_n = 0$ at $V = 0$ and $\alpha_n \to \ln 2$ at $V \to \infty$ for half filling. The interpolation details depend on n and N.

Figure 3 shows $S_n(V)$ for half-filling, calculated from wavefunctions obtained by direct numerical diagonalization. The $S_n(V)$ function evolves from $S_{\mathrm{FF}} = \ln[C(N, n)]$ to $\ln[2C(N, n)] \simeq S_{\mathrm{FF}} + 0.6931$. For $n > 1$, there is an interesting non-monotonic behavior in some cases. At present there is no simple picture of the non-monotonic behavior.

We also see Schrödinger cat physics in the *t-V* model: the $V = +\infty$ ground state is a superposition of two CDW states of the form $|101010\ldots10\rangle$ and $|010101\ldots01\rangle$. The fragility of this cat state can be seen by adding a single-site potential, $\epsilon c_1^\dagger c_1$, or a staggered potential, $\epsilon' \sum_i c_{2i}^\dagger c_{2i}$. The ground state then collapses to a single crystal wavefunction, and S_n drops to $\ln[C(N, n)]$ (figure 3, top panel).

Phase transition. The small-n particle entanglement entropies show no strong signature of the phase transition at $V = 2$, even after extrapolating to the $N \to \infty$ limit. This is not too surprising because the notion of space enters rather weakly in the definition of
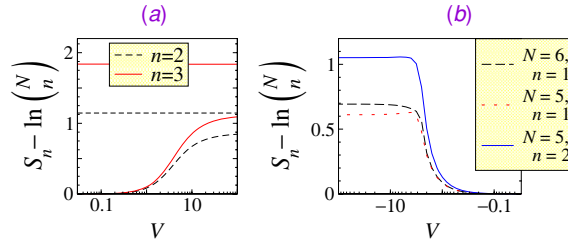
Figure 4. (*a*) S_n for $N = 7$, $L = 12 \neq 2N$. Horizontal lines are corresponding maximal bounds $\ln[C(L, n)]$. (*b*) Negative V, half-filling. Free-fermion contribution $\ln[C(N, n)]$ has been subtracted off in each case.

particle entanglement; thus, S_n is not too sensitive to diverging correlation length or large-scale fluctuations. It remains unclear whether sharper signatures appear for finite n/N (as opposed to $n \ll N$).

Away from half-filling. For $N \neq L/2$, the behavior is qualitatively similar to the half-filled case, α_n increasing from zero to an $\mathcal{O}(1)$ value as V increases from zero to infinity (figure 4(*a*)). However, there is no simple picture for the $V \to \infty$ limit. Also, $\alpha_n(V)$ appears to be monotonic, perhaps because $\alpha_n(V \to \infty)$ is not constrained as in the half-filled (CDW) case.

Note that, except for $S_{n=1}$ in the half-filled case, the particle entanglement never saturates the upper bound, $\ln[C(L, n)]$, dictated by Hilbert space size.

Negative V. An attractive interaction causes the fermions to cluster. In the $V \to -\infty$ limit, the ground state is a superposition (cat state) of L terms, each a cluster of the N fermions. The cat state can be destroyed as in the positive-V case. For half-filling with even N, the $V \to -\infty$ wavefunction yields $S_1 = \ln N + \ln 2$ (figure 4(*b*)). There are $\mathcal{O}(N^{-1})$ corrections for odd $N = L/2$.

5.2. Other fermionic systems

Other than the 1D spinless fermion model (5.1) and the quantum Hall states (section 7), we are not aware of further explicit calculations for fermionic many-particle systems. In [6], calculates particle entanglement of the Hubbard dimer (2-site Hubbard model), and the current authors have found that preliminary numerics on short Hubbard chains show behaviors analogous to the spinless-fermion chain.

6. Hard-core anyons in one dimension

In one and two dimensions, quantum indistinguishable particles need not transform under exchange as fermions or bosons; rather, a continuum of possible intermediate cases connects the boson and fermion cases. Particles with such intermediate statistics are known as *anyons* [23].

A Bethe ansatz solution is available for the anyonic many-particle continuum model with contact interactions, and has recently received renewed attention [24]. The Hamiltonian is

$$H = -\sum_i^N \frac{\partial^2}{\partial x_i^2} + \gamma \sum_{i<j} \delta(x_i - x_j),$$

and the anyonic statistics imposes the condition

$$\Psi^\theta(\dots, x_i, x_{i+1}, \dots) = \exp[\mathrm{i}(\theta - \pi)\epsilon(x_{i+1} - x_i)]\Psi^\theta(\dots, x_{i+1}, x_i, \dots)$$

on the many-body wavefunction. Here $\epsilon(x) = 0$ (or 1) if $x > 0$ ($x < 0$)and θ is the anyonic parameter. For $\theta = 0$ or $\theta = \pi$, this Hamiltonian reduces to free fermions or Lieb–Liniger Bose gas correspondingly. The choice of periodic boundary conditions $\Psi(x_1, \dots, x_i + L, \dots, x_N) = \Psi(x_1, \dots, x_i, \dots x_N)$ constrains the anyonic parameter to be an integer multiple of $2\pi/(N-1)$. Here L is the system size.

The exact solution of the model has been exploited in [12] to calculate the entropy of particle-partitioning entanglement S_1 between $n = 1$ anyon and the rest, in the limit $\gamma \to \infty$. In this limit it is possible to compute the one-particle momentum occupation numbers, $c_N^\theta(j) = 1/L \int_0^L \rho_1(x) \cos(2\pi j x/L)\,\mathrm{d}x$. This in turn allows one to obtain the one-particle entanglement entropy:

$$S_1^\theta(N) = -\sum_{j=-\infty}^\infty c_N^\theta(j) \ln c_N^\theta(j).$$

Here j indexes the momenta, $k_j = 2\pi j/L$. For free fermions ($\theta = 0$), there are N equal non-zero momentum occupation numbers: $c_N^0(j) = 1/N$ for $-(N-1)/2 \leqslant j \leqslant (N-1)/2$. This gives the expected result $S_1^{\theta=0}(N) = \ln N$.

For nonzero θ it is not possible to obtain a closed analytic expression for the $c_N^\theta(j)$. Some asymptotic relations ($j \ll N$) using the Toeplitz determinant form of the one-particle density matrix are provided in [12], but this is not enough to extract the entanglement entropy. We will therefore only review numerical results extracted directly from the exact Toeplitz determinant. A fit to this numerical data (figure 5(a)) indicates that in the limit $N \gg 1$ entanglement entropy behaves as

$$S_1^\theta(N) \simeq \ln N + f(\theta) + \frac{\kappa(\theta)}{\sqrt{N}}.$$

$f(\theta)$ is an N-independent function and describes the main dependence of the one-particle entanglement entropy on the anyonic parameter θ. Figure 5(a) shows some S_1 values calculated numerically, and from this one can extract $f(\theta)$ values, plotted in figure 5(b). The extracted $f(\theta)$ values fit extremely well to a sine function. Explaining this regular behavior of the sub-leading term $f(\theta)$ remains an open and important problem.

The fact that entropy scales as $\ln N$ with a prefactor 1 is expected at $\theta = 0$ and $\theta = \pi$ from the arguments involving fermions and condensation-less bosons, discussed in previous sections. In this sense, the leading $\ln N$ behavior for intermediate values of θ is no surprise. However, from the point of view of the momentum occupation functions $c_N^\theta(j)$, the prefactor 1 is not evident as the $c_N^\theta(j)$ functions are quite nontrivial. For bosons ($\theta = \pi$), the leading $\ln N$ behavior is reported to persist for finite values of the interaction γ [21]. One might therefore expect a leading $\ln N$ at all θ and all $\gamma > 0$, but this has not yet been seen through explicit calculation.
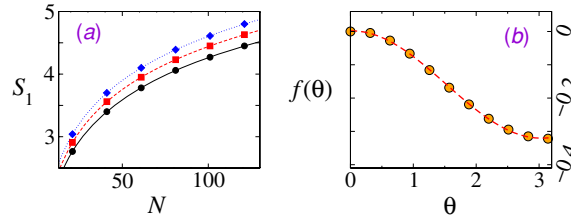
12

Figure 5. (*a*) One-particle entanglement entropy, S_1^θ, as function of *N*, for $\theta = \pi$ (dots fitted by solid line), $\theta = \pi/2$ (squares fitted by dashed line) and for $\theta = \pi$ (diamonds fitted by dotted line). The fits are of form $S_1 \sim \ln N + f(\theta) + \kappa(\theta)/\sqrt{N}$. (*b*) The filled dots are $f(\theta)$ obtained numerically. The dashed line is a sine fit.
(Data: courtesy of Raoul Santachiara.)

7. Fractional quantum Hall states

7.1. Preliminaries

The fractional quantum Hall (FQH) states have long fascinated the condensed-matter community due to their remarkable transport properties and the exotic nature of their quasiparticle excitations [27–30]. Recently there has been enhanced interest in FQH states with *non-Abelian statistics* [28–30] due to the possibility of implementing quantum computation schemes topologically protected from decoherence [31].

The unusual features of FQH states have been notoriously difficult to characterize using traditional condensed-matter concepts such as local order parameters and *n*-point correlation functions. Therefore, using novel measures of quantum correlations, such as entanglement entropies inspired by quantum information theory, is an attractive idea for quantum Hall states. One aspect of fractional quantum Hall states, namely *topological order* [32], has been successfully probed using spatial-partitioning entanglement [8, 9, 33–35]. Here, we will describe particle-partitioning entanglement in FQH states, following mainly [8, 9]. The most striking result is that particle entanglements are closely approximated by upper bounds whose expressions reflect the *exclusion statistics* inherent in FQH states.

We will consider both Abelian and non-Abelian FQH states, &focusing on a paradigmatic example of each class, namely the Laughlin (L) states [27] and the Moore–Read (MR) (or pfaffian) states [28, 36, 37]. In planar geometry, the respective wavefunctions are given by

$$\Psi_L(\{z_i\}) = \prod_{i<j}(z_i - z_j)^m \, e^{-\sum_i |z_i|^2/4}$$

$$\Psi_{MR}(\{z_i\}) = \text{Pf}\left(\frac{1}{z_i - z_j}\right) \prod_{i<j}(z_i - z_j)^m \, e^{-\sum_i |z_i|^2/4},$$

with Pf denoting the antisymmetric Pfaffian symbol, and $z_i = x_i + iy_i$ representing the coordinates of the *i*th particle. The fermionic Laughlin states (odd *m*) describe the physics of the most prominent series of FQH states observed as Hall resistivity plateaus in transport measurements on two-dimensional electron gases in semiconductor heterostructures. The Moore–Read state with $m = 2$ is widely expected to describe the state causing an observed plateau at a Landau-level filling fraction with even denominator. Since quantum statistics plays an important role for particle-partitioning entanglement, we also consider *bosonic* FQH states. These have not yet been realized experimentally, but have been the focus of experimental proposals and efforts with laser-cooled trapped bosonic atoms.
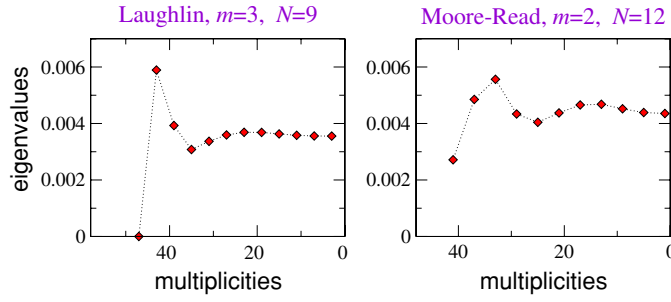
13

Figure 6. Eigenvalues for the 2-particle reduced density matrix, plotted against their multiplicities, for one Laughlin and one Moore-Read state.

We will describe FQH states in a spherical geometry [41]. In this representation the fermions are placed on a sphere containing a magnetic monopole. The magnetic orbitals of the relevant Landau level are then represented as angular momentum orbitals; the total angular momentum is half the number of flux quanta, $L = \frac{1}{2}N_\phi$. The $N_\phi + 1$ orbitals are labeled either $l = 0$ to N_ϕ or $L_z = -L$ to $+L$. For N particles at fractional filling $\nu = 1/m$, one finds the interesting FQH states for $N_\phi = mN - S$, where S is a finite-size shift. The Laughlin states appear at $S = m$ while for the Moore–Read states $S = m + 1$. The 'filling' acquires the usual meaning $\nu = N/N_\phi$ only in the thermodynamic limit. The orbitals each are localized around a 'circle of latitude' on the sphere, with the $l = 0$ orbital localized near one 'pole.'

7.2. Summary of main results

Appreciating that derivations involving FQH states are not readily accessible to readers unfamiliar with the quantum Hall literature, we summarize our main results in this subsection. The technical details are deferred to the remaining subsections.

We consider the entropy of entanglement between n_A particles of the state and the remaining $n_B = N - n_A$ particles. (In this section, we prefer to display the subscript A explicitly because there is a profusion of symbols to distinguish from.)

For both Laughlin and Moore–Read series of states, one can consider how the structure of the FQH wavefunctions reduces the rank of the reduced density matrices ρ_{n_A}. Hence, one can derive upper bounds S_A^{bound} for the particle-entanglement entropy S_{n_A} [8, 9], which are reduced compared to the naive bound (S^F) obtained from the full reduced Hilbert space. For FQH states on the sphere, in the simpler cases ($n_A = 2$) the rank reduction has a physical interpretation in terms of the $SU(2)$ multiplet structure of the spectrum of ρ_{n_A}.

For $n_A \ll N$, these upper bounds in fact happen to be close approximations to the actual values. This is due to the fact that the nonzero eigenvalues of ρ_{n_A} are distributed relatively flatly (figure 6). (The more flat the eigenvalue distribution is, the closer the entanglement entropy is to the upper bound $\ln \mathcal{D}$ dictated by the local Hilbert space dimension $\mathcal{D}$.) This is in sharp contrast to the exponential-like eigenvalue distributions well-known from spatial entanglement [9, 38–40].

The upper bounds are logarithms of combinatorial quantities which reflect the *exclusion statistics* of quasiparticle excitations in FQH states [25]. In addition, these quantities distinguish between the physics of the Laughlin and the Moore–Read states—the fact that the leading correlations have a 2-body nature in the $m = 3$ Laughlin states and a 3-body nature

14

in the $m = 2$ Moore–Read states is reflected in the $1/N$ expansions of the approximations S_A^{bound}.

7.3. Reduced ranks and entanglement upper bounds: fermionic states

For N fermions, n_A particles in the A block, and the total number of orbitals given by $N_\phi + 1 = 2L + 1$, the obvious upper limit S_A^{F} from Hilbert space counting is

$$S_A \leqslant S_A^{\text{F}} = \ln \binom{N_\phi + 1}{n_A}. \tag{6}$$

In the FQH states the correlations are such that the particles avoid each other and the entropy is further reduced. To obtain a handle on this, one may reason as follows. The model FQH states in the Laughlin and Moore–Read series can be characterized as zero-energy eigenstates of a Hamiltonian penalizing pairs and/or triplets of particles coming to the same position. After tracing out the coordinates for the B set, the dependence on those in the A set is such that one still has a zero-energy eigenstate. However, the number of orbitals available to the A particles is larger than what is needed to make the model FQH state in the A sector, and one instead has a certain number of quasi-holes on top of the A set model state. The total ground state degeneracy for this situation has been studied in the literature: see [37] for the Laughlin and Moore–Read states and [42] for the Read–Rezayi [29] and non-Abelian spin singlet (NASS) [30] series of non-Abelian FQH states.

Laughlin states.   The N-particle Laughlin state is realized on a total of $N_\phi + 1$ Landau orbitals, corresponding to $N_\phi = m(N - 1)$ flux quanta. The Laughlin state for n_A particles would need $N_\phi^A = m(n_A - 1)$ flux quanta; we thus have an excess flux of $\Delta N_\phi = N_\phi - N_\phi^A = m(N - n_A)$. This corresponds to the presence of $n_{\text{qh}} = \Delta N_\phi$ quasi-holes over the ground state. According to [37] each of the quasi-holes has a number of $n_A + 1$ effective orbitals to choose from, with bosonic counting rules (meaning that two or more quasi-holes can be in the same effective orbital). This gives a number of quasi-hole states equal to

$$\binom{(n_A + 1) + n_{\text{qh}} - 1}{n_{\text{qh}}} = \binom{n_A + n_{\text{qh}}}{n_A} = \binom{N_\phi + 1 - (m - 1)(n_A - 1)}{n_A},$$

leading to the following upper bound to the entropy S_A:

$$S_A^{\text{bound}} = \ln \binom{N_\phi + 1 - (m - 1)(n_A - 1)}{n_A}. \tag{7}$$

We remark that this expression has a clear interpretation in terms of exclusion statistics [25]: the counting factor in equation (7) gives the number of ways n_A particles can be placed in $N_\phi + 1$ orbitals, in such a way that a particle placed in a given orbital l excludes particles from orbitals l' with $|l - l'| < m$.

Moore–Read.   For the fermionic Moore–Read states at $\nu = 1/m$, with $m = 2, 4, \ldots$, we can reason in a similar way, with now $N_\phi = m(N - 1) - 1$. As for the Laughlin states we have an excess flux of $\Delta N_\phi = N_\phi - N_\phi^A = m(N - n_A)$, but now the number of quasi-holes is twice this number due to the fact that the fundamental quasi-holes correspond to half a flux quantum. Thus, $n_{\text{qh}} = 2\Delta N_\phi$. We now take from [37] the following result for the total quasi-hole degeneracy:

$$\sum_{F \equiv n_A \bmod 2}^{n_A} \binom{n_{\text{qh}}/2}{F} \binom{(n_A - F)/2 + n_{\text{qh}}}{n_{\text{qh}}}. \tag{8}$$

The logarithm of this expression gives us an upper bound S_A^{bound} as before.

Expansion in N^{-1}.   For the Laughlin states, for $n_A \ll N$ we get from equation (7) for large N

$$S_A^{\mathrm{F}} - S_A^{\mathrm{bound}} = \frac{1}{N}\frac{m-1}{m}n_A(n_A-1) + \mathcal{O}(1/N^2).$$

We compare this to the $m = 2$ Moore–Read states:

$$S_A^{\mathrm{F}} - S_A^{\mathrm{bound}} = \frac{1}{N^2}\frac{3}{4}n_A(n_A-1)(n_A-2) + \cdots.$$

The leading deviation from S_A^F is a 3-body term at order $1/N^2$. This result nicely illustrates the fact that the leading correlations in the $m = 2$ Moore–Read state have a 3-body character: the wave-function vanishes if at least three particles come to the same position.

For $m \neq 2$ the leading correlations do have a 2-body character, as for the Laughlin states:

$$S_A^{\mathrm{F}} - S_A^{\mathrm{bound}} = \frac{1}{N}\frac{m-2}{m}n_A(n_A-1) + \cdots.$$

Other fermionic FQH sequences.   The quasi-hole counting rules for the order-k clustered spin-polarized (Read–Rezayi [29]) and spin-singlet (NASS [30]) states are all known in the literature [42]. They can be used to generalize the upper bounds on particle-entanglement entropy given in this subsection to these more intricate non-Abelian FQH states.

Bosonic quantum Hall states.   We consider bosonic Laughlin states at filling fraction $\nu = \frac{1}{m}$ with $m = 2, 4, \ldots,$. The naive upper bound to the entropy associated with placing n_A bosons in $N_\phi + 1$ orbitals is

$$S_A^{\mathrm{B}} = \ln\binom{N_\phi + n_A}{n_A}.$$

The expression for S_A^{bound} remains unchanged from the fermionic Laughlin case, giving the following leading correction in a $1/N$ expansion:

$$S_A^{\mathrm{B}} - S_A^{\mathrm{bound}} = \frac{1}{N}n_A(n_A-1) + \cdots. \tag{9}$$

For a bosonic Moore–Read state, with filling fraction $\nu = 1/m$ with $m = 1, 3, \ldots,$, the leading $1/N$ correction becomes

$$S_A^{\mathrm{B}} - S_A^{\mathrm{bound}} = \frac{1}{N}\frac{m-1}{m}n_A(n_A-1) + \cdots. \tag{10}$$

In the case $m = 1$, the leading correlations have 3-body character, resulting in the vanishing of the leading $1/N$ correction. (Similar to the fermionic $m = 2$ MR states.)

Multiplet picture for rank reduction.   For $n_A = 2$, we can get a simple picture of the reduction of the entanglement entropy (or of the rank of the reduced density matrix) compared to the naive bound, through consideration of multiplet structures present in the eigenspectrum of ρ_{n_A}. For FQH states on a sphere, the n_A-particle reduced density matrices ρ_{n_A} commute with the total angular momentum operators $\mathbf{L}_{n_A}^2$ and $L_{n_A}^z$ of the selected n_A particles. As a result, the eigenvalues of ρ_{n_A} are organized in $SU(2)$ multiplet structures: an eigenvalue for total angular momentum L_{n_A} will be $(2L_{n_A} + 1)$-fold degenerate.

For $n_A = 2$ fermions, each having angular momentum $L = \frac{1}{2}N_\phi$, the 2-particle states have total angular momenta $L_2 = 2L - 1, 2L - 3, \ldots, 1\,(0)$, for L integer (half-integer),

giving a total number of $(2L + 1)(2L)/2$ states. This corresponds to the naive upper bound to the entanglement entropy:

$$S_{n_A=2} \leqslant \ln\left[(2L+1)(2L)/2\right] = \ln\binom{N_\phi + n_A}{n_A}. \tag{11}$$

Inspecting the explicit structure of the fermionic Laughlin states with $m = 3, 5, \ldots$, one finds that the eigenvalues corresponding to 2-particle states with $L_2 = 2L - 1, 2L - 3, \ldots,$ $2L - (m - 2)$ all vanish. The reason is that the correlations in the Laughlin states are such that particles cannot come too close together. For example, if a first fermion occupies the $l = 0$ orbital, localized near the north pole, the Laughlin wavefunction has zero amplitude for finding a second fermion in orbitals $l = 1, l = 2, \ldots, l = m - 1$. The highest possible value of the angular momentum of the two fermions combined is thus $L_2 = L + (L - m)$. The remaining number of non-zero eigenvalues is $(2L + (2 - m))(2L + (1 - m))/2$, leading to an improved bound on the entropy $S_{n_A=2}$:

$$S_{n_A=2} \leqslant \ln[(2L + (2-m))(2L + (1-m))/2], \tag{12}$$

which is clearly the $n_A = 2$ case of equation (7).

For $n_A > 2$, the multiplet structures are more complicated, and it is difficult to generalize the above argument, but one expects that the arguments of the previous subsection, relying on the quasihole degeneracy, are equivalent to the vanishing of one or more eigenvalue multiplets.

7.4. Numerical results

Reduced spectra.   In deriving the upper bound S_A^{bound} we relied on the fact that a certain number of eigenvalues of the reduced density matrix vanish. The bounds would be exact if all non-zero eigenvalues were equal, but there is some eigenvalue spread, the bounds overestimate the actual values for the entropies.

Figure 6 plots the eigenvalues for the $n_A = 2$ reduced density matrix, for $N = 9$ particles on a sphere in the $m = 3$ Laughlin state ($L = 12$). The horizontal axis represents the degeneracy $2L_2 + 1$ of the eigenvalues, in descending order. The eigenvalue at $L_2 = 2L - 1 = 23$, with degeneracy 47, vanishes; the non-zero eigenvalues show some scatter around an asymptotic value. Due to this scatter the entropy $S = 5.509$ is somewhat lower than the upper bound $S_A^{\text{bound}} = 5.533$.

An important difference between the $m = 3$ Laughlin and the $m = 2$ Moore–Read states is the absence of vanishing eigenvalues for the 2-particle reduced density matrix. The eigenvalue distribution shown in figure 6 (right) illustrates this point.

In the $m = 2$ Moore–Read state, there are vanishing eigenvalues in the reduced density matrix of $n_A \geqslant 3$ particles. The number of nonzero eigenvalues predicted by equation (8) agrees with numerical results. For example, for $n_A = 3$ and $N = 10$ particles there are 770 nonvanishing eigenvalues, in agreement with equation (8).

While the nonzero eigenvalues are not all equal, their distributions are quite flat, in sharp contrast to the near-exponential eigenvalue distributions for spatial partitioning.

Entanglement entropy values.   In figure 7 we compare numerically computed particle-entanglement entropies with the bounds described above.

Note that for the $m = 2$ Moore–Read case, S_A^{bound} coincides with S_A^{F} for $n_A = 2$ (dashed and solid lines coincide in the lower-left panel of figure 7), which can be inferred from equation (8) and is also reflected in the fact that none of the eigenvalue multiplets vanish in that particular case (figure 6, right panel).
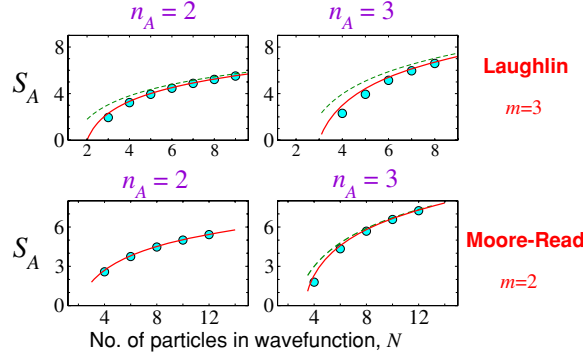
17

Figure 7. Particle-entanglement entropies. Laughlin ($m = 3$) state in upper panels, Moore–Read ($m = 2$) state in lower panels. Dots are numerical exact values, the dotted line represents S_A^F (equation (6)) and the solid curves are the bound S_A^{bound} (equation (7) for upper panels and equation (8) for lower panels).

7.5. Reduced density matrices and correlation functions

Since the n_A-particle reduced density matrices ρ_{n_A} are obtained by integrating out all but n_A of the particles, one expects these matrices to be related to the n_A-particle correlation functions. For $n_A = 2$, [9] provides a detailed explanation of this relationship, more specific than the general discussion of subsection 3.5.

In particular, the $n_A = 2$ eigenvalue distributions are indeed very closely related to the two-particle correlation function $g_2(r)$. In fact, the $g_2(r)$ curve may be regarded as simply a continuous form of the λ_l versus descending-$(2l + 1)$ curves of figure 6. This explains why the eigenvalue distributions of $\rho_{n_A=2}$ in figures 6, although discrete, are reminiscent of the well-known $g_2(r)$ curves for Laughlin and Moore–Read states.

8. Calogero–Sutherland model

The Calogero–Sutherland model holds a special place in condensed matter theory as an exactly solvable model which possesses fractional excitations [43]. The model has Jastrow-type ground state wavefunctions similar to FQH wavefunctions; the eigenfunctions are known in terms of Jack polynomials. Using the properties of Jack polynomials ('duality relations'), [11] has studied particle-partitioning entanglement entropies for this model.

The model is described by the Hamiltonian ($0 \leqslant x \leqslant L$)

$$\hat{H} = -\frac{1}{2}\sum_{i=1}^{N}\frac{\partial^2}{\partial x_i^2} + \sum_{i<j}\frac{\beta(\beta-1)\left(\frac{\pi}{L}\right)^2}{\sin^2\left(\frac{\pi}{l}(x_i - x_j)\right)}.$$

By utilizing properties of Jack polynomials in the limit $N - n \to \infty$, [11] provides the following upper bound on the n-particle entanglement entropy S_n in the N-particle Calogero–Sutherland ground state:

$$S_n \leqslant S_n^{bound} = \ln\binom{\beta(N-n)+n}{n}.$$

In close analogy to the FQH results discussed in section 7, this expression can be interpreted in terms of exclusion statistics. Tracing out one particle is equivalent to removing one particle

18

from Fermi sea, which in turns creates β quasiholes. Thus, taking out $N-n$ particles creates $\beta(N-n)$ quasiholes. There are $C(\beta(N-n)+n, n)$ ways to accommodate n particles and $\beta(N-n)$ quasiholes within the Fermi sea, which gives the above estimate.

An explicit expression for the sub-leading correction to this bound is also given in [11]:

$$S_N \simeq \ln\left(\frac{(\beta(N-n)+n)!}{n!(\beta(N-n))!}\right) - n(\ln\beta - 1 + \beta^{-1}) + \mathcal{O}(N^{-1}).$$

In this formula the first term originates from the number of nonzero eigenvalues whereas the second one comes from the asymptotic eigenvalue distribution. An explicit expression for the $\mathcal{O}(N^0)$ term is possible because of the more detailed understanding of the eigenvalue distribution (in terms of the relevant Young tableaus) that is available for this model, as compared to the FQH case.

9. Conclusions

Particle entanglement is an emerging important measure of correlations in itinerant many-particle quantum systems. In this review, we have provided an extremely simple and explicit example (section 2) designed to clarify the concept and remove misconceptions. We have synthesized the available results into a set of general observations (section 3). We have pointed out several different mechanisms for particle entanglement in itinerant quantum states, such as absent or imperfect Bose condensation, anti-symmetrization of fermionic systems and Schrödinger cat states.

The bulk of this review (section 4 onwards), of course, surveys the available results on particle entanglement in itinerant many-body systems. The discussion of more conventional bosonic, fermionic and even anyonic systems, falls mostly within the general observations of section 3, with more subtle effects (e.g. anyonic statistics) showing up as sub-leading terms. The study of particle partitioning in quantum Hall states and the Calogero–Sutherland model provides a window into more exotic phenomena, such as exclusion statistics.

Clearly, the study of particle-partitioning entanglement is at its infancy, and one expects further insights and new calculations to appear. We hope that this review will provide inspiration for further advances.

Acknowledgments

References

[1] Schliemann J, Cirac J I, Kuś M, Lewenstein M and Loss D 2001 *Phys. Rev.* A **64** 022303
[2] Paškauskas R and You L 2001 *Phys. Rev.* A **64** 042310
[3] Omar Y, Paunković N, Bose S and Vedral V 2002 *Phys. Rev.* A **65** 062305
[4] Zeng B, Zhai H and Xu Z 2002 *Phys. Rev.* A **66** 042324
[5] Wiseman H M and Vaccaro J A 2003 *Phys. Rev. Lett.* **91** 097902
[6] Dowling M R, Doherty A C and Wiseman H M 2006 *Phys. Rev.* A **73** 052323
[7] Iblisdir S, Latorre J I and Orus R 2007 *Phys. Rev. Lett.* **98** 060402
[8] Haque M, Zozulya O and Schoutens K 2007 *Phys. Rev. Lett.* **98** 060401

  [9] Zozulya O S, Haque M, Schoutens K and Rezayi E H 2007 *Phys. Rev.* B **76** 125310
[10] Zozulya O S, Haque M and Schoutens K 2008 *Phys. Rev.* A **78** 042326
[11] Katsura H and Hatsuda Y 2007 *J. Phys. A: Math. Theor.* **40** 13931
[12] Santachiara R, Stauffer F and Cabra D 2007 *J. Stat. Mech.* L05003
[13] Santachiara R and Calabrese P 2008 arXiv:0802.1913v1
[14] Amico L, Fazio R, Osterloh A and Vedral V 2008 *Rev. Mod. Phys.* **80** 517
[15] Eisert J, Cramer M and Plenio M B 2008 arXiv:0808.3773
[16] Horodecki R, Horodecki P, Horodecki M and Horodecki K 2009 *Rev. Mod. Phys.* **81** 865
[17] Lacroix C 2009 *Phys. B: Phys. Condens. Matter* **404** 3038
[18] Mueller E J, Ho T-L, Ueda M and Baym G 2006 *Phys. Rev.* A **74** 033612
[19] Yang C N 1962 *Rev. Mod. Phys.* **34** 694
[20] Lieb E H and Liniger W 1963 *Phys. Rev.* **130** 1605
[21] Calabrese P personal communication, unpublished
[22] Walker L R 1959 *Phys. Rev.* **116** 1089
      Bonner J C and Fisher M E 1964 *Phys. Rev.* **135** A640
[23] Leinaas J M and Myrheim J 1977 *Nuovo Cimento* B **37** 1
      Wilczek F 1982 *Phys. Rev. Lett.* **49** 957
      Khare A 2005 *Fractional Statistics and Quantum Theory* (Singapore: World Scientific)
[24] Kundu A 1999 *Phys. Rev. Lett.* **83** 1275
      Batchelor M T, Guan X-W and Oelkers N 2006 *Phys. Rev. Lett.* **96** 210402
      Batchelor M T and Guan X-W 2006 *Phys. Rev.* B **74** 195121
      Batchelor M T, Guan X-W and He J-S 2007 *J. Stat. Mech.* P03007
      Pâtu O I, Korepin V E and Averin D V 2007 *J. Phys. A: Math. Theor.* **40** 14963
[25] Haldane F D M 1991 *Phys. Rev. Lett.* **67** 937
[26] Yang C N and Yang C P 1966 *Phys. Rev.* **151** 258
[27] Tsui D C, Stormer H L and Gossard A C 1982 *Phys. Rev. Lett.* **48** 1559
      Laughlin R B 1983 *Phys. Rev. Lett.* **50** 1395
[28] Moore G and Read N 1991 *Nucl. Phys.* B **360** 362
[29] Read N and Rezayi E 1999 *Phys. Rev.* B **59** 8084
[30] Ardonne E and Schoutens K 1999 *Phys. Rev. Lett.* **82** 5096
[31] Kitaev A Yu 2003 *Ann. Phys.* **303** 2
      Freedman M, Larsen M and Wang Z 2002 *Commun. Math. Phys.* **227** 605
      Bonesteel N E *et al* 2005 *Phys. Rev. Lett.* **95** 140503
      Das Sarma S, Freedman M and Nayak C 2005 *Phys. Rev. Lett.* **94** 166802
[32] Wen X G and Niu Q 1990 *Phys. Rev.* B **41** 9377
      Wen X G 1989 *Phys. Rev.* B **40** 7387
      Wen X G 1990 *J. Math. Phys.* **4** 239
      Wen X G 1990 *Phys. Rev.* B **41** 12838
      Wen X G 1991 *Phys. Rev.* B **44** 2664
      Wen X G 2004 *Quantum Field Theory of Many-Body Systems* (Oxford: Oxford University Press)
      Oshikawa M and Senthil T 2006 *Phys. Rev. Lett.* **96** 060601
      Alet F, Walczak A M and Fisher M P A 2006 *Physica* A **369** 122
[33] Kitaev A and Preskill J 2006 *Phys. Rev. Lett.* **96** 110404
      Levin M and Wen X G 2006 *Phys. Rev. Lett.* **96** 110405
[34] Li H and Haldane F D M 2008 *Phys. Rev. Lett.* **101** 010504
[35] Zozulya O, Haque M and Regnault N 2009 *Phys. Rev.* B **79** 045409
[36] Read N 2001 *Physica* B **298** 121
[37] Read N and Rezayi E 1996 *Phys. Rev.* B **54** 16864
[38] Calabrese P and Lefevre A 2008 *Phys. Rev.* A **78** 032329
[39] Chung M C and Peschel I 2000 *Phys. Rev.* B **62** 4191
[40] Peschel I, Kaulke M and Legeza O 1999 *Ann. Phys.* **8** 153
[41] Haldane F D M 1983 *Phys. Rev. Lett.* **51** 605
[42] Gurarie V and Rezayi E 2000 *Phys. Rev.* B **61** 5473
      Ardonne E, Read N, Rezayi E and Schoutens K 2001 *Nucl. Phys.* B **607** 549
      Ardonne E 2002 *J. Phys. A: Math. Gen.* **35** 447
[43] Calogero F 1969 *J. Math. Phys.* **10** 2191
      Sutherland B 1971 *Phys. Rev.* A **4** 2019